Harnessing the Potential of Omnidirectional Multi-Rotor Aerial Vehicles in Cooperative Jamming Against Eavesdropping

Daniel Bonilla Licea[1,2], Hajar El Hammouti[1], Giuseppe Silano[2], and Martin Saska[2]

***Abstract*—Recent research in communications-aware robotics has been propelled by advancements in 5G and emerging 6G technologies. This field now includes the integration of Multi-Rotor Aerial Vehicles (MRAVs) into cellular networks, with a specific focus on under-actuated MRAVs. These vehicles face challenges in independently controlling position and orientation due to their limited control inputs, which adversely affects communication metrics such as Signal-to-Noise Ratio. In response, a newer class of omnidirectional MRAVs has been developed, which can control both position and orientation simultaneously by tilting their propellers. However, exploiting this capability fully requires sophisticated motion planning techniques. This paper presents a novel application of omnidirectional MRAVs designed to enhance communication security and thwart eavesdropping. It proposes a strategy where one MRAV functions as an aerial Base Station, while another acts as a friendly jammer to secure communications. This study is the first to apply such a strategy to MRAVs in scenarios involving eavesdroppers.**

***Index Terms*—UAVs, multi-rotor systems, communication-aware robotics, jamming, eavesdropper, physical layer security**

I. Introduction

Recent interest in communications-aware robotics has surged, evidenced by an increasing number of publications [1], [2]. This promising field has largely been propelled by advancements in 5G and the development of 6G technologies. These innovations aim to integrate Multi-Rotor Aerial Vehicles (MRAVs) into cellular communications networks to boost performance [3]–[5].

A significant portion of this research focuses on under-actuated MRAVs [6]–[8]. Such MRAVs [9], which can hover at specific positions and track trajectories, are pivotal for functions like mobile communications relays or aerial Base Stations (BSs) [10], [11]. However, their primary limitation lies in the inability to independently control both position and orientation. This constraint arises from the fact that under-actuated MRAVs typically have fewer control inputs, which include thrust, roll and pitch angles, and yaw rate [12], than the number of Degree of Freedoms (DoFs) needed for fully autonomous position and orientation control [9]. This restricts the optimization of aerial communications networks as effective signal reception depends on both the MRAV's position and its orientation.

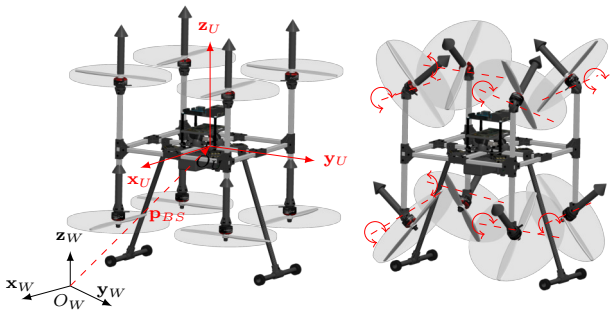

Figure 1: Illustration of two MRAV configurations along with the global ($\mathcal{F}_W$) and untilted ($\mathcal{F}_U$) reference systems: under-actuated (left) and omnidirectional (right) [13]. Arcs represent the rotation direction of servos used for varying the thrust vector.

In contrast, omnidirectional MRAVs overcome these limitations by enabling simultaneous control over position and orientation [13], [14]. This is achieved by actively tilting their propellers using servo motors, optimizing energy consumption by aligning propeller spinning directions with the required orientation [15], [16]. This balance between dexterity and energy efficiency supports various task-specific demands and can effectively counteract challenges like jamming attacks or eavesdropping [17]. Figure 1 illustrates both under-actuated and omnidirectional configurations of an MRAV, illustrating the versatility of these platforms.

The present study expands on the capabilities of omnidirectional MRAVs by exploring their use in scenarios involving eavesdroppers. This paper introduces an innovative approach where a team of omnidirectional MRAVs, one acting as an aerial Base Station and the other as a friendly jammer,

[1]Daniel Bonilla Licea and Hajar El Hammouti are with the College of Computing, Mohammed VI Polytechnic University, Ben Guerir, Morocco (emails: {daniel.bonilla, hajar.elhammouti}@um6p.ma).

[2]Daniel Bonilla Licea, Giuseppe Silano, and Martin Saska are with the Czech Technical University in Prague, Czech Republic (emails: {bonildan, silangiu, martin.saska}@fel.cvut.cz).

This work was partially funded by the European Union under the project Robotics and Advanced Industrial Production (reg. no. CZ.02.01.01/00/22_008/0004590), by the Czech Science Foundation (GAČR) under research project no. 23-07517S, and by CTU grant no SGS23/177/OHK3/3T/13.

collaboratively work to secure communications for legitimate users while disrupting nearby eavesdroppers. This strategy, which leverages advanced motion planning techniques, represents a novel application to enhance the security of MRAV communications in the presence of eavesdroppers.

The focus of this research is the joint optimization of both position and orientation (also known as pose) of omnidirectional MRAVs, marking the first instance, to the best of the authors' knowledge, of employing such a strategy to ensure secure communications in the presence of eavesdroppers. Previous research has demonstrated the use of MRAVs for secure communications, such as using a single MRAV equipped with an antenna array to simultaneously support legitimate communications and jam eavesdroppers [18]. Another study [19] examined a dual-MRAV network where one MRAV collects data from users, and the other jams eavesdroppers, optimizing trajectories and power for maximum secrecy. In scenarios like [20], MRAVs transmit private messages and jamming signals to protect communications, optimizing power and trajectory for the highest secrecy rates. Similarly, [21] explores two MRAVs working together to transmit secure information to a ground node while jamming eavesdroppers. Other research, such as [22], considers the impact of environmental factors like wind on MRAV stability and communication efficacy, optimizing systems against worst-case scenarios. However, none of the mentioned approaches address enhancing secrecy rates by physically orienting the antennas in such a way that jamming signals are directed at eavesdroppers and while information signals are directed at legitimate users, this is achieved by leveraging the omnidirectional capabilities and it is an alternative to the use of traditional beamforming.

Our work builds on these studies by using a dual-MRAV setup with cooperative jamming, utilizing omnidirectional MRAVs' ability to direct signals efficiently, thereby increasing secrecy rates and enhancing network security. This innovative application appears to be the first of its kind in utilizing omnidirectional MRAVs for improved network security.

II. System model

We consider the scenario where a team of two MRAVs is charged with providing secure and efficient communication to various ground users in the presence of N eavesdroppers. One MRAV (MRAV-I) communicates with the ground nodes while the other MRAV (MRAV-J) protects the privacy of the communication by jamming eavesdroppers in the region.

A. Eavesdroppers and legitimate users

We assume that MRAV-I transmits information to legitimate stationary nodes, and this transmission is vulnerable to interception by malicious eavesdroppers. To address this, the team of MRAVs handles one legitimate node at a time using Temporal Division Multiple Access (TDMA)[1]. Therefore, we focus on the system during a single time slot, denoting S_0 as the active legitimate user at that time, and we will denote $\{S_j\}_{j=1}^{N}$ as the set of eavesdroppers. We represent the coordinates in the global reference frame $\mathcal{F}_W = \{O_W, \mathbf{x}_W, \mathbf{y}_W, \mathbf{z}_W\}$ of the node S_j as $\mathbf{p}_{S_j} \in \mathbb{R}^3$ (see Figure 1). Without loss of generality, we assume that $\mathbf{p}_{S_0} = \mathbf{0}$, with $\mathbf{0} \in \mathbb{R}^3$. We also assume that all eavesdroppers and legitimate users are equipped with single omnidirectional antennas. To ensure secure transmission between MRAV-I and the user S_0, during its allotted time slot, the MRAV-J emits artificial noise to disrupt the eavesdroppers.

B. Omnidirectional MRAVs

We consider both MRAVs are omnidirectional. The position of the MRAV-i ($i \in \{I, J\}$) in the global reference frame $\mathcal{F}_W$ is denoted as $\mathbf{p}_{U_i} \in \mathbb{R}^3$. Additionally, we introduce an i-th untilted coordinate frame $\mathcal{F}_{U_i} = \{O_{U_i}, \mathbf{x}_{U_i}, \mathbf{y}_{U_i}, \mathbf{z}_{U_i}\}$, which is aligned with the global coordinate frame $\mathcal{F}_W$ and centered at $\mathbf{p}_{U_i}$ (see Figure 1). To precisely describe the orientation of MRAV-i in the global coordinate frame $\mathcal{F}_W$, we use Euler angles, specifically roll (φ_i), pitch (ϑ_i), and yaw (ψ_i). We refer to the orientation of MRAV-i as $\boldsymbol{\eta}_i = [\varphi_i, \vartheta_i, \psi_i]^\top \in \mathbb{R}^3$.

The omnidirectional MRAV-i is equipped with a single antenna, which is located at $\mathbf{p}_{U_i}$, on its upper surface and oriented according to the following vector expressed in $\mathcal{F}_{U_i}$:

$$\boldsymbol{\Upsilon}_i(\boldsymbol{\eta}_i) = \begin{bmatrix} \cos(\varphi_i)\sin(\vartheta_i)\cos(\psi_i) + \sin(\varphi_i)\sin(\psi_i) \\ \cos(\varphi_i)\sin(\vartheta_i)\sin(\psi_i) - \sin(\varphi_i)\cos(\psi_i) \\ \cos(\varphi_i)\cos(\vartheta_i) \end{bmatrix}. \quad (1)$$

We also consider that the MRAVs experience slight jittering due to the wind and other control issues. To account for this jittering, we follow the same model as [23] which adds the jittering to the orientation vector: $\boldsymbol{\eta}_i = \boldsymbol{\eta}_i^d + \boldsymbol{w}_i(t)$, where $\boldsymbol{\eta}_i^d \in \mathbb{R}^3$ represents the desired Euler angles for the MRAV-i, and $\boldsymbol{w}_i(t) \in \mathbb{R}^3$ is a zero-mean Gaussian random process with covariance matrix $\mathbf{C}_i = \sigma_{U_i}^2 \mathbf{I}_3$, where $\mathbf{I}_3 \in \mathbb{R}^{3\times 3}$ is the identity matrix and $\sigma_{U_i}^2$ is the variance. For notational simplicity we assume the same variance for all three Euler angles, note that this simplification does not affect our proposed method. We write the joint Probability Density Function (PDF) of the three components of $\boldsymbol{w}_i(t)$ as $f_{w_i}(\varphi_i, \vartheta_i, \psi_i) = g(\varphi_i; \sigma_{U_i}^2) g(\vartheta_i; \sigma_{U_i}^2) g(\psi_i; \sigma_{U_i}^2)$, where $g(\cdot; \sigma_{U_i}^2)$ is a Gaussian distribution of zero-mean and variance $\sigma_{U_i}^2$. We also assume that $\boldsymbol{w}_I(t)$ and $\boldsymbol{w}_J(t)$ are statistically independent and identically distributed random variables.

[1]We assume the time slots are sufficiently long to allow the team of MRAVs to position themselves optimally for each legitimate node and transmit data for an extended duration before moving to the next legitimate user.

C. Channel model

We consider both MRAVs' antennas to be dipoles. As a result, the normalized power radiation patterns of the information and jammer MRAVs can be characterized as follows [24]:

$$G(\gamma) = \sin^2(\gamma), \tag{2}$$

where γ is the elevation angle component of the Angle of Departure (AoD) of the antenna in consideration. Now, let us consider the communications link between MRAV-i and node S_j. The cosine of the elevation angle component for this communication link can be expressed as:

$$\cos(\gamma_{ij}) = \left\langle \frac{\mathbf{p}_{S_j} - \mathbf{p}_{U_i}}{\|\mathbf{p}_{S_j} - \mathbf{p}_{U_i}\|}, \boldsymbol{\Upsilon}(\boldsymbol{\eta}_i) \right\rangle, \tag{3}$$

where $\langle \cdot, \cdot \rangle$ represents the inner product operation, and γ_{ij} is the elevation angle of the AoD between MRAV-i and node S_j. Subsequently, we can formulate the radiation pattern of the antenna of MRAV-i as:

$$G(\gamma_{ij}) = 1 - \left\langle \frac{\mathbf{p}_{S_j} - \mathbf{p}_{U_i}}{\|\mathbf{p}_{S_j} - \mathbf{p}_{U_i}\|}, \boldsymbol{\Upsilon}(\boldsymbol{\eta}_i) \right\rangle^2. \tag{4}$$

We assume that the air-to-ground channel is mainly influenced by path loss [22]. Additionally, we suppose that the MRAVs know the location of the legitimate node and have estimates of the locations of the eavesdroppers[2]; we denote those estimates as $\{\hat{\mathbf{p}}_{S_j}\}_{j=1}^N$. We also assume that the MRAVs do not know the variance of the estimates nor their statistical distributions. The distance between MRAV-i and node S_j is $d_{ij} \triangleq \|\mathbf{p}_{S_j} - \mathbf{p}_{U_i}\|$, and the Signal-to-Interference-plus-Noise Ratio (SINR) at node S_j is:

$$\Gamma_j = \frac{G(\gamma_{Ij}) P_I d_{Ij}^{-2}}{G(\gamma_{Jj}) P_J d_{Jj}^{-2} + \sigma_j^2}, \ \forall j \in \{0, \dots, N\}, \tag{5}$$

where P_i is the transmit power of MRAV-i, and σ_j^2 is the variance of additive white Gaussian noise of node j. Finally, the secrecy rate, calculated with the estimated positions of the eavesdroppers, is:

$$R(\boldsymbol{\Gamma}) = B \left[\log_2(1 + \Gamma_0) - \max_{j \in \{1,\dots,N\}} (\log_2(1 + \hat{\Gamma}_j)) \right]^+, \tag{6}$$

where $[\cdot]^+ = \max(0, \cdot)$, B represents the allocated bandwidth, $\boldsymbol{\Gamma} = [\Gamma_0, \hat{\Gamma}_1, \dots, \hat{\Gamma}_N]^\top$, and $\{\hat{\Gamma}_j\}_{j=1}^N$ are the estimated SINR at the eavesdroppers obtained by using the estimated positions $\{\hat{\mathbf{p}}_{S_j}\}_{j=1}^N$ instead of the real ones $\{\mathbf{p}_{S_j}\}_{j=1}^N$.

[2]The locations of the eavesdroppers can be estimated, for instance, as described in [25] and then shared with the MRAVs.

III. Problem Formulation

We aim to optimize the desired pose (position and orientation) of the information MRAV and the jamming MRAV, along with their transmission powers, to maximize the secrecy rate of the legitimate user S_0. This problem is stated as follows:

$$\underset{\boldsymbol{\eta}_I^d, \mathbf{p}_{U_I}, \boldsymbol{\eta}_J^d, \mathbf{p}_{U_J}, P_I, P_J}{\text{maximize}} \quad \mathbb{E}[R(\boldsymbol{\Gamma})] \tag{7a}$$

$$\text{s.t.} \quad \underline{z} \leq \mathbf{e}_3^\top \mathbf{p}_{U_i} \leq \bar{z}, \tag{7b}$$

$$\left\| \begin{bmatrix} \mathbf{I}_2 & \\ & 0 \end{bmatrix} \boldsymbol{\eta}_i \right\|_\infty \leq \frac{\pi}{2}, \tag{7c}$$

$$0 \leq P_i \leq \bar{P}, \tag{7d}$$

$$\text{with } \psi_i = 0, \ \forall i \in \{I, J\}. \tag{7e}$$

In this formulation, the objective function (7a) represents the expected value (accounting for disturbances in the MRAVs orientation) of the secrecy rate for the user S_0 (see (6)):

$$\mathbb{E}[R(\boldsymbol{\Gamma})] = \iiiint_{\mathbb{R}^4} R(\boldsymbol{\Gamma}) \prod_{i=\{J,I\}} g(\varphi_i; \sigma_{U_i}^2) g(\vartheta_i; \sigma_{U_i}^2) \mathrm{d}\varphi_i \mathrm{d}\vartheta_i. \tag{8}$$

Constraint (7b) restricts the altitude of the MRAVs within specified limits, denoted as $\underline{z}$ and $\bar{z}$. Here, $\mathbf{e}_3 = (0, 0, 1)^\top$ corresponds the third column of the identity matrix $\mathbf{I}_3$. Constraint (7c) defines permissible ranges for the pitch (ϑ) and roll (φ) angles, with $\mathbf{I}_2 \in \mathbb{R}^{2\times 2}$. The optimization problem explores a search space with twelve dimensions, encompassing the position of both MRAVs $\{\mathbf{p}_{U_i}\}_{i=\{J,I\}}$, their roll and pitch angles $\{\varphi_i, \vartheta_i\}_{i=\{J,I\}}$ as well as their transmission powers $\{P_i\}_{i=\{J,I\}}$. Notably, we omit consideration of the yaw angle (ψ) (7e) due to the omnidirectional radiation pattern of the antenna, which exhibits uniformity around its axis. Lastly, constraint (7d) enforces that the transmission powers P_i remain strictly positive and do not exceed a maximum value denoted as $\bar{P}$.

The resulting optimization problem (7) is non-convex and features non-smooth and nonlinear functions, such as the $[\cdot]^+$ and $\max(\cdot)$ functions in (6). This makes it challenging to find a global optimal solution. Therefore, we will introduce a novel approach to decompose the problem (7) into simpler subproblems, ultimately deriving a suboptimal solution.

IV. Solution

In the proposed approach, we tackle the optimization problem in four distinct phases which are executed iteratively, and they are described individually in the next subsections.

A. Phase 1: MRAV-I orientation

In this section, we introduce the concept of the *maximum gain plane* for the MRAV-i, with $i \in \{I, J\}$, and explain how it is used to determine the orientation of the

MRAV-I. This plane, denoted as $\mathcal{X}_i$, is defined as follows: $\mathcal{X}_i = \{\mathbf{q} + \mathbf{p}_{U_i} : \mathbf{q} \times \boldsymbol{\Upsilon}(\boldsymbol{\eta}_i^d) = 0, \mathbf{q} \in \mathbb{R}^3\}$. This plane represents the region where the antenna of MRAV-i achieves maximum gain, assuming the orientation is set to the desired one, $\boldsymbol{\eta}_i^d$. Additionally, we define the *ground plane* as $\mathcal{G}$, consisting of points in $\mathcal{F}_W$ with zero height above the ground: $\mathcal{G} = \{[x, y, 0]^\top : x, y \in \mathbb{R}\}$. Before determining the MRAV-I orientation, we introduce a line denoted as $\mathcal{L}_i$. This line is the intersection of $\mathcal{X}_i$ and $\mathcal{G}$ (i.e., $\mathcal{L}_i = \mathcal{X}_i \cap \mathcal{G}$.) and is determined based on the position of MRAV-I ($\mathbf{p}_{U_I}$).

Figure 2 depicts the overall scenario, and the orientation of the MRAV-I is chosen to satisfy two criteria:

- *Criterion* 1 *(Maximum antenna gain)* Ensure that the maximum antenna gain of the MRAV-I is directed towards the legitimate user, i.e., $\mathbf{p}_{S_0} \in \mathcal{L}_I$.
- *Criterion* 2 *(Horizontal distance)* Maximize the horizontal distance between $\mathcal{L}_I$ and the eavesdroppers to minimize the gain of MRAV-I's antenna observed by the eavesdroppers.

The line $\mathcal{L}_I$ can be represented as the set: $\mathcal{L}_I = \{[x,\, y,\, 0]^\top : y = ax, x \in \mathbb{R}\}$, with $a \in \mathbb{R}$ being a parameter to be optimized. To find the optimal a, we define a vector $\mathbf{w}$ that is orthonormal to $\mathcal{L}_I$: $\mathbf{w} = [-a, 1,\ 0\ ]^\top \left(\sqrt{1+a^2}\right)^{-1}$.

Given that $\mathbf{p}_{S_0} = \mathbf{0}$, we already satisfy Criterion 1 regardless the value of a. To satisfy Criterion 2, we optimize the parameter a to maximize the minimum distance between the eavesdroppers and the line $\mathcal{L}_I$. The minimum distance, denoted as H_i, between S_i and $\mathcal{L}_I$, is given by: $H_i = |\mathbf{w}^\top \mathbf{p}_{S_i}|$.

Thus, we formulate the optimization problem as maximizing the minimum value of $\hat{H}_i^2 = |\mathbf{w}^\top \hat{\mathbf{p}}_{S_i}|^2$ by varying the parameter a of the vector $\mathbf{w}$. To avoid numerical issues associated with an unbounded search space for a, we use the parameter ν defined as $a = \tan(\nu)$ with $\nu \in [-\pi/2, +\pi/2]$. Note that this implies that $\nu = \pi/2$ and $\nu = -\pi/2$ both correspond to a vertical line and are treated equivalently. Therefore, the optimization problem becomes[3]:

$$\underset{a}{\text{maximize}} \left(\min_{j=\{1,\ldots,N\}} \hat{H}_j^2 \right). \tag{9}$$

The optimization problem (9) is non-convex and can have multiple local maxima and minima. The number of local maxima and minima are proportional to the number of eavesdroppers N and also depends on their angular locations relative to S_0. To address this, we can employ numerical optimization techniques such as simulated annealing, which can handle non-convex problems with multiple local optima efficiently when the search space is bounded. Once we have determined $\mathcal{L}_I$, we can calculate the desired orientation of MRAV-I, as:

$$\boldsymbol{\eta}_I^d = \begin{bmatrix} -\text{asin}\left([\boldsymbol{\Upsilon}(\boldsymbol{\eta}_I^d)]_y\right) \\ \arctan 2\left(\frac{[\boldsymbol{\Upsilon}(\boldsymbol{\eta}_I^d)]_x}{\cos\left(\text{asin}\left([\boldsymbol{\Upsilon}(\boldsymbol{\eta}_I^d)]_y\right)\right)}, \frac{[\boldsymbol{\Upsilon}(\boldsymbol{\eta}_I^d)]_z}{\cos\left(\text{asin}\left([\boldsymbol{\Upsilon}(\boldsymbol{\eta}_I^d)]_y\right)\right)}\right) \\ 0 \end{bmatrix}, \tag{10}$$

where $\text{asin}(\cdot)$ is the arcsine function, $\arctan 2(x, y)$ is the four quadrants inverse tangent, and:

$$\boldsymbol{\Upsilon}(\boldsymbol{\eta}_I^d) = \left(\frac{\ell_1 - \mathbf{p}_{U_I}}{|\ell_1 - \mathbf{p}_{U_I}|_2}\right) \times \left(\frac{\ell_2 - \mathbf{p}_{U_I}}{|\ell_2 - \mathbf{p}_{U_I}|_2}\right), \tag{11}$$

where ℓ_1 and ℓ_2 are any two points in $\mathcal{L}_I$, and $[\boldsymbol{\Upsilon}(\boldsymbol{\eta}_I^d)]_x$, $[\boldsymbol{\Upsilon}(\boldsymbol{\eta}_I^d)]_y$, and $[\boldsymbol{\Upsilon}(\boldsymbol{\eta}_I^d)]_z$ represent the x, y, and z components of the vector $\boldsymbol{\Upsilon}(\boldsymbol{\eta}_I^d)$, respectively. This orientation ensures that the MRAV-I provides maximum antenna gain in the direction of the legitimate user while providing low antenna gain in the direction of eavesdroppers.

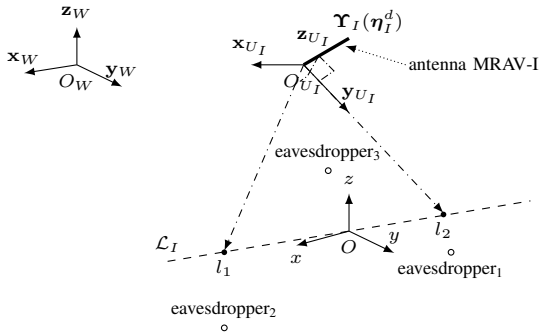

Figure 2: A schematic representation of the $\mathcal{X}_i$ and $\mathcal{G}_i$ planes along with the eavesdroppers, the legitimate user (located at the origin O), and the MRAV-I.

B. Phase 2: MRAV-J orientation

Regarding the MRAV-J orientation, we propose orienting it to minimize its interference to the legitimate user S_0:

$$\boldsymbol{\Upsilon}(\boldsymbol{\eta}_J^d) = \frac{\mathbf{p}_{S_0} - \mathbf{p}_{U_I}}{\|\mathbf{p}_{S_0} - \mathbf{p}_{U_I}\|_2}. \tag{12}$$

Then $\boldsymbol{\eta}_J^d$ is extracted from $\boldsymbol{\Upsilon}(\boldsymbol{\eta}_J^d)$ using the same formula (10) after replacing $\boldsymbol{\Upsilon}(\boldsymbol{\eta}_I^d)$ with $\boldsymbol{\Upsilon}(\boldsymbol{\eta}_J^d)$. If the MRAV-J experienced no jittering, then $\boldsymbol{\Upsilon}(\boldsymbol{\eta}_J) = \boldsymbol{\Upsilon}(\boldsymbol{\eta}_J^d)$, and thus the null of the antenna of the MRAV-J would be permanently oriented to the legitimate user. Consequently, the MRAV-J could radiate as much power as possible without interfering with the receiver of the legitimate user. However, due to the jittering, the legitimate user will receive some small amount of power from the MRAV-J, which will slightly degrade its SINR.

[3]Note that we are using the estimated locations of the eavesdroppers.

C. Phase 3: Transmission Power

With the orientations of both MRAV-I and MRAV-J determined as functions of their positions, we proceed by substituting (11)–(12) expressions into the original optimization problem (7). The resultant problem is formulated as follows:

$$\underset{\mathbf{p}_{U_I},\mathbf{p}_{U_J},P_I,P_J}{\text{maximize}} \quad \mathbb{E}[R(\mathbf{\Gamma})] \tag{13a}$$

$$\text{s.t.} \quad \underline{z} \leq \mathbf{e}_3^\top \mathbf{p}_{U_i} \leq \bar{z}, \tag{13b}$$

$$0 \leq P_i \leq \bar{P}, \tag{13c}$$

$$(11), (12). \tag{13d}$$

It should be noted that directly optimizing the secrecy rate presents challenges due to the flat valleys introduced by the nonlinear function $[\cdot]^+ = \max(0, \cdot)$ in $R(\mathbf{\Gamma})$. To mitigate this issue, the utility function is adjusted by replacing $R(\mathbf{\Gamma})$ with:

$$\hat{R}(\mathbf{\Gamma}) = B\left[\log_2(1+\Gamma_0) - \max_{j\in\{1,\ldots,N\}}(\log_2(1+\hat{\Gamma}_j))\right]. \tag{14}$$

Additionally, computing the fourth-dimensional integral (7) numerically is computationally demanding. Therefore, instead of numerically evaluating the integral to obtain the expected value over the jittering, a Monte Carlo approach is adopted. Various realizations of the Euler angles ($\boldsymbol{\eta}$) for both MRAVs are generated according to the Gaussian model considered for the jittering, the secrecy rate is computed for each realization, and then averaged. By generating a sufficiently large number of realizations, the mean closely approximates the expected value, making this method computationally efficient.

D. Phase 4: Position Optimization

Upon computing the expression for the secrecy rate as outlined in Section IV-C, a numerical method is employed to solve the optimization problem concerning the 3D positions of both MRAVs and their transmission powers. Specifically, an interior point search method [26] is utilized to efficiently handle the constrained optimization (13) with the modified optimization target (14). Once the optimal positions and powers are obtained, they are reintroduced into the initial problem (7), as described in Sections IV-A and IV-B, to determine the optimal orientations for the updated positions and powers. This iterative process continues until a predefined number of iterations is reached or convergence is achieved.

V. Simulations

In this section, we evaluate the performance of our technique under different conditions. Firstly, we examine the scenario where the MRAVs operate without experiencing any jitter, followed by an assessment of the performance of our suboptimal solution (see Sections IV-C and IV-D). Additionally, we compare the effectiveness of the omnidirectional MRAVs with under-actuated ones in this context. Finally, we investigate the impact of jittering on the system's performance.

A. Simulation Setup

To evaluate our proposed approach, we consider an area of $1000\,\mathrm{m} \times 1000\,\mathrm{m}$ with a legitimate user positioned at the origin. We study the scenario where 2 eavesdroppers are randomly distributed within this area. Both the information and jammer MRAVs are initially placed within the region, with altitudes ranging from $80\,\mathrm{m}$ to $300\,\mathrm{m}$ ($\underline{z}$ and $\bar{z}$). We assume that the MRAVs transmit with a maximum power $\bar{P}$ within the range of $\bar{P} \in [0.1, 1.1]\,\mathrm{W}$. The noise variance for both legitimate users and eavesdroppers is set to $\sigma_l = \sigma_e = 10^{-12}\,\mathrm{W}$. The allocated bandwidth for each MRAV is $B = 1\,\mathrm{MHz}$.

To assess our approach, we compare it against the following benchmarks: *1) Interior-point method*: Solves the optimization problem described in (7) with respect to (w.r.t.) all optimization variables, including the orientations, positions, and powers of the MRAVs, using the interior-point method. *2) Conventional MRAV*: Assumes under-actuated MRAVs with fixed orientation and employs the interior-point method to optimize the MRAVs positions and transmit powers.

B. Simulation Results

Figure 3 illustrates the optimal 3D positions of MRAV-I and MRAV-J, along with lines $\mathcal{L}_I$ and $\mathcal{L}_J$, representing the direction of maximum gain of the antennas.

As depicted in the figure, the maximum gain of the antenna of the MRAV-I for all approaches is strategically directed towards the legitimate user to ensure efficient communication. Conversely, the orientation of the maximum gain of the antenna for the cooperative jammer, $\mathcal{L}_J$, is distinctly oriented away from the legitimate user and directed towards the eavesdroppers. It is also important to note that the $\mathcal{L}_I$ obtained by our proposed approach always intersects with the legitimate user, ensuring that the maximum gain of the antenna of the MRAV-I is always directed to the legitimate user, contributing to the maximization of the secrecy rate.

Figure 4a presents the secrecy rate plotted against the maximum power for both our proposed approach and the two benchmarks without any jittering on the MRAVs orientation and with perfect knowledge of the eavesdroppers position. As seen in the figure, our proposed approach achieves a significant performance compared to the interior-point method. This substantial gain arises from the non-convexity of the secrecy rate function, whereby the interior-point method may become trapped in a local optimum, significantly deviating from the optimal performance. Moreover, the figure shows

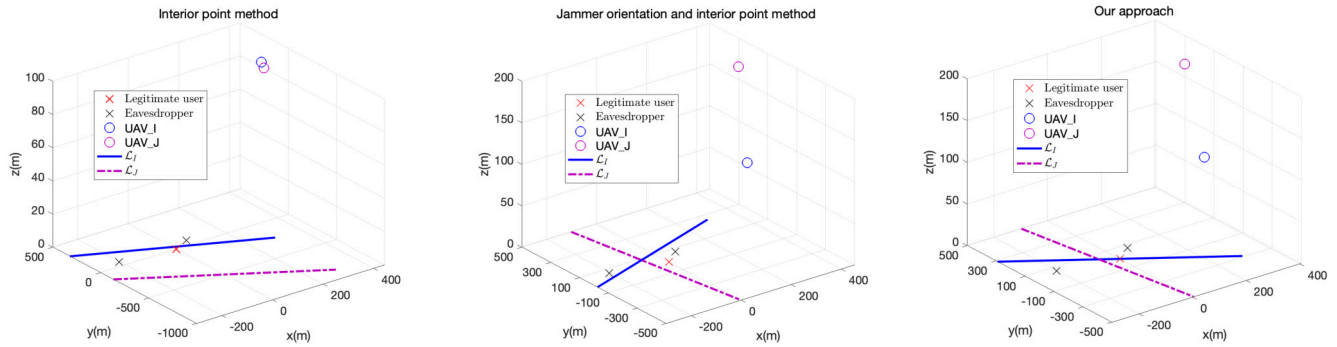

(a) Interior Point. (b) Jammer Orientation. (c) Our Approach.

Figure 3: Final 3D positions obtained using the interior-point method, combined jammer orientation and interior-point method, and our proposed approach for scenarios with 2 eavesdroppers.

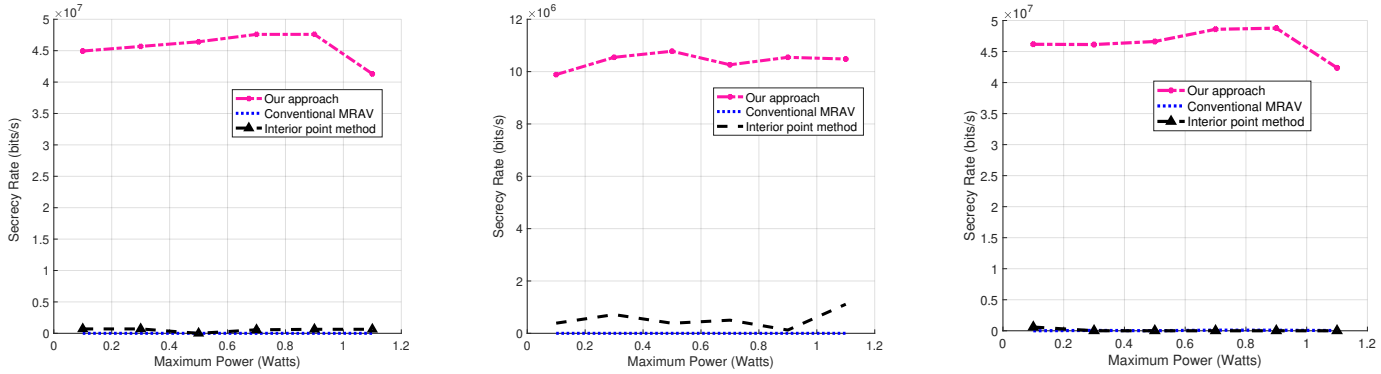

(a) Without jittering and uncertainty. (b) With jittering. (c) With uncertainty about the eavesdropper's position.

Figure 4: Secrecy rate as a function of maximum power.

that the conventional MRAV approach exhibits the poorest performance due to its inability to optimize antenna orientation, resulting in very low performance.

Figures 4b and 4c illustrate the impact of jittering and uncertainty about the eavesdroppers position on the secrecy rate obtained by our approach and the benchmarks. In Figure 4b, we examine the scenario where we optimize the expectation of the secrecy rate over jittering but test for a random jittering value. Whereas, in Figure 4c, we optimize the secrecy rate with an estimated value of the eavesdroppers position and test for a random value of their positions. As shown in the figure, our proposed approach outperforms the benchmarks for both scenarios, followed by interior-point method.

VI. Conclusions

In this paper, we explored the application of teams of omnidirectional MRAVs to enhance the secrecy rate among legitimate nodes. We leveraged the unique capacity of omnidirectional MRAVs to independently control their position and orientation. Our investigation demonstrated that by utilizing this capability of omnidirectional MRAVs and integrating cooperative jamming techniques, we can substantially enhance the security of communications with legitimate nodes in environments containing multiple malicious eavesdroppers. To the

best of authors' knowledge, this study represents the initial endeavor to employ such MRAVs in addressing these types of problems. However, numerous inquiries persist regarding the utilization of these MRAVs in other physical layer security scenarios. We contend that these inquiries present novel research avenues within the communications community.

REFERENCES

[1] D. Bonilla Licea *et al.*, "Communication-Aware Energy Efficient Trajectory Planning With Limited Channel Knowledge," *IEEE Transactions on Robotics*, vol. 36, no. 2, pp. 431–442, 2020.

[2] Q. Wu *et al.*, "Joint Trajectory and Communication Design for Multi-UAV Enabled Wireless Networks," *IEEE Transactions on Wireless Communications*, vol. 17, no. 3, pp. 2109–2121, 2018.

[3] D. Bonilla Licea *et al.*, "When Robotics Meets Wireless Communications: An Introductory Tutorial," *Proceedings of the IEEE*, vol. 112, no. 2, pp. 140–177, 2024.

[4] A. Muralidharan *et al.*, "Communication-Aware Robotics: Exploiting Motion for Communication," *Annual Review of Control, Robotics, and Autonomous Systems*, vol. 4, pp. 115–139, 2021.

[5] D. Bonilla Licea *et al.*, "Optimum Trajectory Planning for Multi-Rotor UAV Relays with Tilt and Antenna Orientation Variations," in *European Signal Processing Conference*, 2021, pp. 1586–1590.

[6] J. H. Jung *et al.*, "Multi-robot path finding with wireless multihop communications," *IEEE Communications Magazine*, vol. 48, no. 7, pp. 126–132, 2010.

[7] H. El Hammouti *et al.*, "Air-to-ground channel modeling for UAV communications using 3D building footprints," in *Ubiquitous Networking: 4th International Symposium*. Springer, 2018, pp. 372–383.

[8] M. Calvo-Fullana *et al.*, "Communications and Robotics Simulation in UAVs: A Case Study on Aerial Synthetic Aperture Antennas," *IEEE Communications Magazine*, vol. 59, no. 1, pp. 22–27, 2021.

[9] M. Hamandi *et al.*, "Design of multirotor aerial vehicles: A taxonomy based on input allocation," *The International Journal of Robotics Research*, vol. 40, no. 8-9, pp. 1015–1044, 2021.

[10] D. Bonilla Licea *et al.*, "Communications-Aware Robotics: Challenges and Opportunities," in *International Conference on Unmanned Aircraft Systems*, 2023, pp. 366–371.

[11] M. Kishk *et al.*, "Aerial Base Station Deployment in 6G Cellular Networks Using Tethered Drones: The Mobility and Endurance Tradeoff," *IEEE Vehicular Technology Magazine*, vol. 15, no. 4, pp. 103–111, 2020.

[12] T. P. Nascimento *et al.*, "Position and attitude control of multi-rotor aerial vehicles: A survey," *Annual Reviews in Control*, vol. 48, pp. 129–146, 2019.

[13] Y. Aboudorra *et al.*, "Modelling, Analysis, and Control of OmniMorph: an Omnidirectional Morphing Multi-rotor UAV," *Journal of Intelligent & Robotic Systems*, vol. 110, no. 21, pp. 1–14, 2024.

[14] M. Allenspach *et al.*, "Design and optimal control of a tiltrotor micro-aerial vehicle for efficient omnidirectional flight," *The International Journal of Robotics Research*, vol. 39, no. 10–11, pp. 1305–1325, 2020.

[15] M. Ryll *et al.*, "A Novel Overactuated Quadrotor Unmanned Aerial Vehicle: Modeling, Control, and Experimental Validation," *IEEE Transactions on Control Systems Technology*, vol. 23, no. 2, pp. 540–556, 2015.

[16] ——, "FAST-Hex—A Morphing Hexarotor: Design, Mechanical Implementation, Control and Experimental Validation," *IEEE Transactions on Mechatronics*, vol. 27, no. 3, pp. 1244–1255, 2022.

[17] D. Bonilla Licea *et al.*, "Omnidirectional Multi-Rotor Aerial Vehicle Pose Optimization: A Novel Approach to Physical Layer Security," in *IEEE International Conference on Acoustics, Speech and Signal Processing*, 2024, pp. 9021–9025.

[18] H. Wu *et al.*, "Energy-Efficient and Secure Air-to-Ground Communication With Jittering UAV," *IEEE Transactions on Vehicular Technology*, vol. 69, no. 4, pp. 3954–3967, 2020.

[19] R. Zhang *et al.*, "Dual-UAV Enabled Secure Data Collection With Propulsion Limitation," *IEEE Transactions on Wireless Communications*, vol. 20, no. 11, pp. 7445–7459, 2021.

[20] H. Lee *et al.*, "UAV-Aided Secure Communications With Cooperative Jamming," *IEEE Transactions on Vehicular Technology*, vol. 67, no. 10, pp. 9385–9392, 2018.

[21] C. Zhong *et al.*, "Secure UAV Communication With Cooperative Jamming and Trajectory Control," *IEEE Communications Letters*, vol. 23, no. 2, pp. 286–289, 2019.

[22] Y. Xu *et al.*, "Joint Resource and Trajectory Optimization for Security in UAV-Assisted MEC Systems," *IEEE Transactions on Communications*, vol. 69, no. 1, pp. 573–588, 2021.

[23] W. Chen *et al.*, "Adaptive Hybrid Beamforming for UAV mmWave Communications against Asymmetric Jitter," *IEEE Transactions on Wireless Communications*, pp. 1–14, 2024.

[24] D. B. Miron, "Chapter 2 - antenna fundamentals i," in *Small Antenna Design*, D. B. Miron, Ed. Newnes, 2006, pp. 9–41.

[25] A. Mukherjee *et al.*, "Detecting passive eavesdroppers in the MIMO wiretap channel," in *IEEE International Conference on Acoustics, Speech and Signal Processing*, 2012, pp. 2809–2812.

[26] S. P. Boyd *et al.*, *Convex optimization*. Cambridge university press, 2004.